# Subsea gas plumes and dispersion above sea

A. Huser
*Det Norske Veritas AS, Oslo, Norway*

T. Bengherbia
*Det Norske Veritas Inc. London, UK*

P. Skjetne & J.E. Olsen
*Sintef AS, Trondheim, Norway*

W. Postvoll
*Gassco AS, Hugesund, Norway*

ABSTRACT: The paper presents both state-of-the-art CFD modeling techniques for subsea gas bubble plumes and the subsequent dispersion above sea, and simplified look-up tables where the consequences in terms of distance to flammable gas clouds caused by a subsea gas release are found. Gas transfer from sea to air on the surface (the bubblezone) represents the interface also between separate CFD models for below and above sea. Sintefs CFD models of subsea bubble plumes captures the transient plume behavior, surface dynamics (height of boiling zone, shear layers, radial flow), subsea mass and heat transfer, and it gives transient and stationary boundary conditions for dispersion above sea. It is currently validated for a 10 m water depth experiment. A DNV RP is developed for CFD modeling of dispersion above sea including bubble zone definitions, standard *k-e* model and recommendations for the buoyancy turbulence model, air inlet boundary conditions, and how to maintain turbulence downwind. Different commercial CFD codes are often not able to predict the same plume lengths due to default modeling differences, and the current RP gives the modeling details that need to be followed in order to give consistent results. The CFD generated look-up tables are integrated into a tool called PlumePro where the height and distance to the LFL plume can be found given sea depth, release rate and wind speed. PlumePro interpolates in the look-up tables generated from a set of CFD modeling runs where the state-of-art modeling techniques are applied.

## 1 INTRODUCTION

The paper presents combined work during the last 6 years from SINTEF and DNV where the subsea phenomenon has been considered by SINTEF, and the atmospheric dispersion by DNV. Prediction capabilities for these phenomenon using standard CFD tools is at best variable and available validation experiments and detailed model testing is applied to develop and improve CFD models. The need for improvement of such prediction capabilities is eminent in offshore QRA and safety analyses for; subsea installation, maintenance operations, emergency preparedness, as well as in the event of an accident or during accident investigation.

Commonly so called integral models have been used to study sub-sea release of oil and gas. A few examples of CFD applied to bubble plumes in aeration of lakes or reservoirs have been published, but all of these regardless of release depth have all considered only small release rates typically < 1kg/s. SINTEF has developed a CFD model that can overcome the numerical problems associated with large release rates and which can thus be used to study realistic release rates for offshore applications. In particular the model has been employed to survey gas plume behavior as a function of depth and release rate, and to tabulate the resulting surface plume radius and surface flux profile.

In order to couple the bubble plume simulations with prediction of atmospheric dispersion and estimation of e.g. contours of 50% LEL under different weather conditions, a common format of the parameters to describe gas release on the sea surface is suggested ensuring a consistent approach. When modeling atmospheric dispersion from subsea gas releases using different CFD codes, large discrepancies in the plume lengths were observed even when the codes were using the "standard" k-e turbulence model. In the paper, comparisons are made with chimney release measurements resulting in a set of recommended turbulence parameters, which give the best fit. Default values of these turbulence parameters vary between commercial CFD codes, which explain the differences. Using the recommended settings, consistency is obtained between the different CFD codes. The paper also highlights the important modeling issues which need to be considered when modeling atmospheric dispersion using CFD tools. Finally, a set of CFD cases are presented and tabulated in a way that can be applied to quickly estimate hazard distances.

## 2 SUBSEA GAS PLUMES

Dispersion of gas in the sea can be quantitatively described by mathematical models for ocean bubble plumes. Traditionally this is performed by so-called integral models where the profile of gas fraction and plume velocity is described by Gaussian profiles. A full 3D model has recently been developed to describe the ocean plumes (Cloete, Olsen and Skjetne, 2009, and Skjetne & Olsen, 2012). The model is based on an Eulerian-Lagrangian modeling concept accounting for gas dissolution to the sea water. From this modeling concept it is possible to extract surface data applicable to modeling of atmospheric dispersion of gas.

### 2.1 *Modeling Concept*

The coupled Volume of Fluid (VOF) and Discrete Phase Model (DPM) apply the VOF model to describe the fluid behaviour of the sea water, the gas in the atmosphere and the interface between them. This is an Eulerian two-fluid model with interphase tracking. Since the VOF model cannot resolve the bubbles with an affordable grid resolution, a Lagrangian method, DPM, is used to track the bubbles. The Lagrangian bubbles are connected to the Eulerian phases with a two-way coupling through interchange terms such as the drag force in the respective momentum equations.

The bubbles are modelled as discrete particles without particle-particle interaction. This is carried out with a *Discrete Particle Model* (DPM) which tracks the bubbles with a Lagrangian momentum equation:

$$\frac{d\mathbf{u}_b}{dt} = \frac{\mathbf{g}(\rho_b - \rho)}{\rho_b} + \mathbf{F}_D(u - u_b) + \mathbf{F}_{VM} + \mathbf{F}_L + \mathbf{F}_{TD} \qquad (1)$$

Five forces are normally accounted for: buoyancy, drag, lift, virtual mass and turbulent dispersion. These are the four first terms on the right hand side of the equation. The fifth force is turbulent dispesion. Turbulent dispersion is an additional drag force due to the velocity fluctuations in a turbulent flow. The standard drag force only accounts for drag due to the average velocity field. Turbulent dispersion creates a random addition to the liquid velocity of the drag force in Eq.(2). The random velocity is accounted for by a *random walk model* (Gosman & Ioannides, 1983). It results in a wider plume. Further details on the modelling concept are described in Cloete et.al. (2009a) and Cloete et al. (2009b).

In order to validate the model, modeling results have been compared to experimental results (Engebretsen *et al*., 1997). A series of experiments were conducted in a rectangular basin with a depth of 6.9 m and a surface area of 6 x 9 m. The basin was filled with water and air was released at the bottom at gas rates of 83, 170 and 750 Nl/s (equivalent to 50, 100 and 450 l/s referred to the state at the inlet). Comparison without a lift force gave good agreement with experiments regarding velocity profiles, rise times and fountain height (Cloete *et.al*, 2009b). Velocity profiles based on modelling and experiments are compared in Figure 1 for a chosen gas rate.

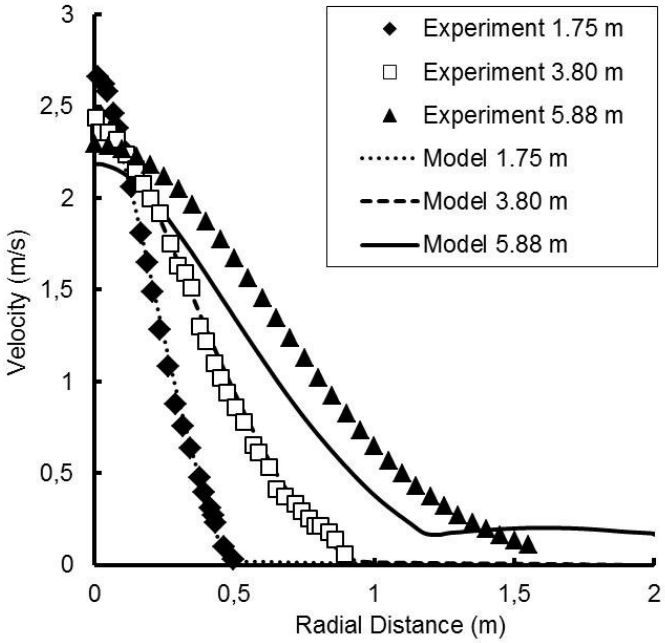


Figure 1: Modelling results of velocity profiles of the liquid phase at different heights above gas release point compared with experiments at a gas rate of 170 Nl/s.

### 2.2 *Gas dissolution*

At larger depths the effect of gas dissolution becomes important. This needs to be accounted for by the model. Since natural gas is often dominated by a large percentage of methane, pure methane gas is considered. The driving force of the mass transfer mechanism responsible for the gas dissolution is the concentration difference of the specific gas component at the bubble surface and in the surrounding liquid. The concentration at the bubble surface is given by the solubility of the gas species and thus the mass flux, $J$, is given by

$$J_i = k_i\left(C_i^{sol} - C_i^{w}\right) \qquad (2)$$

where $k_i$, is the mass transfer coefficient of species $i$ and the concentrations $C$ are given in kg/m$^3$. The total mass transfer $\dot{m}$ accounts for bubble surface area A by $\dot{m} = AJ$.

Different expressions exist for the mass transfer coefficient depending on whether one may assume a clean bubble surface or one contaminated by surfactants. Clean surfaces are mobile and a resulting internal circulation in the bubble due to the forces acting upon the bubble surface is normally significant. This circulation enhances the mass transfer. Surfactants will immobilize the surface and slow down the internal circulation and thus reduce the mass transfer. Further details are given by Skjetne and Olsen (2012).

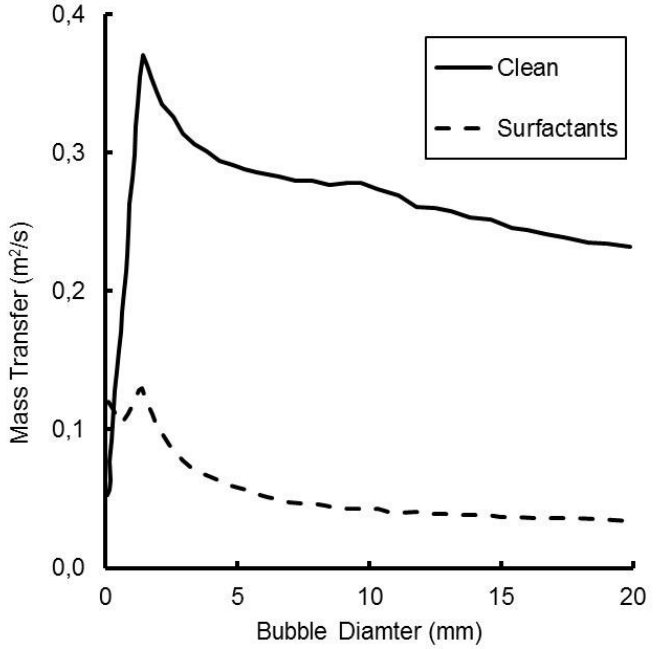


Figure 2: Mass transfer coefficient for methane bubbles with clean and contaminated surface.

The discrepancy in mass transfer from a clean bubble and a surfactant pollutes bubble is illustrated in Figure 2 where the mass transfer coefficient is plotted for different bubble sizes rising with the corresponding terminal velocity Whether the bubbles in a large gas release are affected by surfactants are still open for debate, so both options are included.

The resulting surface flux from two simulations is seen in Figure 3. From a depth of 100 meter a release with a gas rate of 500 kg/s were studied with the option of either mass transfer from a clean bubble or from a rigid bubble contaminated by surfactants. We see that the surfactant contaminated bubbles gives the highest surface flux, which is the most conservative estimate in terms of safety precautions for surface operations. This is consistent with the results of Figure 2 showing a lower mass transfer coefficient for contaminated bubbles. Mass transfer formulas for the surfactant contaminated bubbles are thus used in safety assessments.

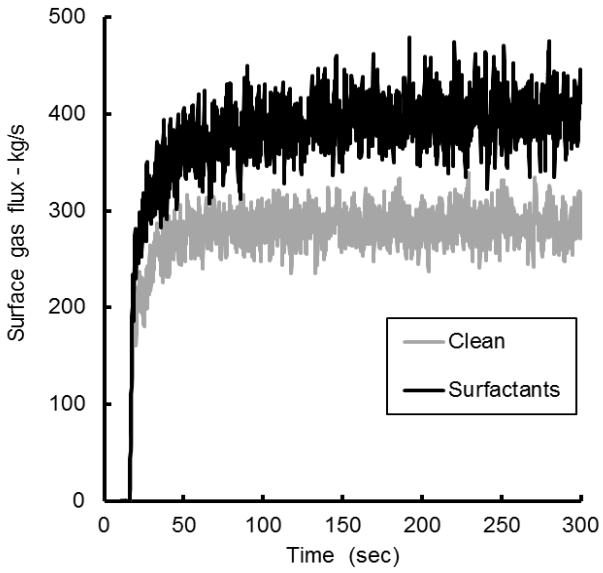


Figure 3: Surface flux as function of time from initial release of 500 kg/s from a depth of 100 meter for clean and surfactant contaminated bubbles.

## 3 DISPERSION ABOVE SEA

### 3.1 *k – ε Turbulence model differences*

It is found that differences in the weighting of the production of dissipation due to buoyancy (Expressed by the parameter $C_{3\varepsilon}$) in the $k-\varepsilon$ turbulence models of FLACS and KFX significantly influence the predicted gas plume lengths and heights, see Figure 4. In the present work (DNV 2010, 2011), this has been shown for a larger number of cases, including also simulations with CFX. An example case is shown in Figure 4 indicating that the differences are large for low wind speed when the buoyancy term becomes dominating. For higher wind speeds, above 5 m/s, the differences are not significant.

The CFD codes tested (FLACS, KFX, and CFX) apply the $k-\varepsilon$ turbulence model, but the default weighting of dissipation production by buoyancy is mainly performed in two different ways in the three codes. KFX and CFX apply approximately the same weighing (KFX_$C_{3\varepsilon}$= 1), whereas FLACS uses a separate weighting (FLACS_$C_{3\varepsilon}$= 0.8). Note that the terms for buoyancy production of dissipation are written differently in FLACS compared to KFX and CFX so that the parameter $C_{3\varepsilon}$ has different definitions in the two models. In effect, the numerical relation between the weighting factors is 5 to 1.

Simulated centre plume trajectories obtained with different weighting of buoyancy has been compared to experimental observations (Briggs 1969) of chimney stack plumes in cross wind (Figure 5). This comparison indicates that the parameter value used in KFX and CFX is best suited for predictive simula-

tions of atmospheric dispersion of a buoyant gas. It is therefore recommended to modify the parameter FLACS_$C_{3\varepsilon}$ from default 0.8 to 0 when modelling dispersion above sea in FLACS. Note that such modification of the FLACS code is not recommended for other applications as the code has not been validated for that.

In the present work, a check of the ability of all three codes (FLACS, KFX and CFX) to reproduce each other's results with the corresponding turbulence settings is performed. It is found that the codes gives similar result as long as the turbulence parameter $C_{3\varepsilon}$ are modelling the same strength of production of

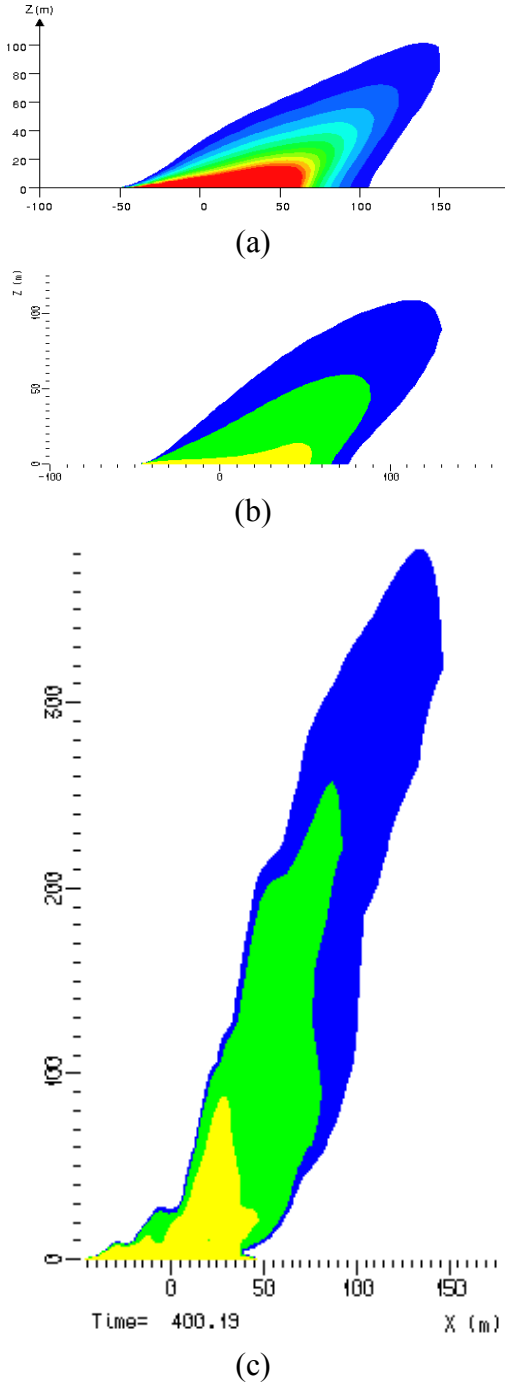


Figure 4. Comparing gas clouds for (a), FLACS with default turbulence parameters; (b), KFX using C3e as in FLACS; and (c) KFX using default turbulence parameters (recommended). All cases with Release rate 450 kg/s, Wind speed 1 m/s, Pasquill stability class D.

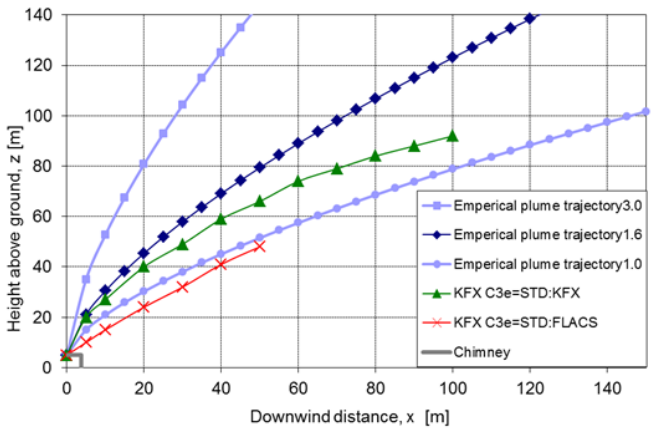


Figure 5. Comparison of the default KFX and FLACS implementations of the standard $k$ – ε turbulence model KFX. Release: 42 kg/s, wind speed: 1 m/s. The factors 3, 1.6 and 1 indicates upper, center and lower bounds of experimental observations, respectively.

dissipation, provided also the boundary conditions are equal and resolution is sufficient.

Differences mainly in the wind inlet boundary conditions, the source term of gas bubbling up on the sea surface, and the ability of the code to maintain atmospheric turbulence downwind are also influencing the dispersion patterns and cloud lengths. A best practice report (DNV 2010) and a DNV Recommended Practice (DNV 2013) are written in order to define these modelling practices. A highlight of this is given in the next section.

### 3.2 *Bubble zone definition*

Release boundary conditions for gas bubbling up at the sea surface are given by a flux distributed over an area. The flux can be given as a top-hat profile or as a two-dimensional Gaussian profile. The area is normally circular, and the radius of the release is depending on the sea depth. If it is a transient release, then the radius is also depending on the "age" of the plume.

The release from the sea can be modelled as a top-hat profile instead of a Gaussian profile without losing significant accuracy in the plume lengths. Test simulations performed in this report indicates that if

*Tophat radius = 0.64 times the Bubblezone radius, or*

*Tophat radius = 1.6 times the standard deviation of the Gaussian distribution of the flux,*

then the plume distances are the same, or within a small deviation, typically 5%.

With these relations, the visible bubble zone has typically a

*Bubble zone radius = 2.5 times the standard deviation of the Gaussian distribution.*

The bubble zone radius is based on CFD results of subsea plumes from Sintef (2009). The Gaussian distribution gives a mass flow of gas of 98% of the total flow within this radius. For larger radius than 2.5 standard deviations, the integrated flux up from the sea is 2% of the total flow of gas.

The bubble zone radius is specified by the area where bubbles are observed coming up. The border is not a sharp circle, however observations from Sintefs CFD simulations and real subsea gas leaks indicates that the border is quite well defined. When the release is modelled as a Gaussian distribution, the bubble zone radius can hence be defined where the integrated flux is reduced to 98% of the total flux.

When the real subsea release is deep enough, a Gaussian distributed flux of gas up from the bubble zone will be established. The release area can be modelled as a flux directed upward with a low velocity, or the added mass of gas can be added as a source to the mass equation in the first cell above the sea inside the bubble zone or top-hat area. If a top-hat radius is applied, the constant flux from the release is simply

$U_g = \dot{m} / \rho A$ (m/s),

Where $A$ is the top hat area of the release ($m^2$), $\rho$ is the release gas density ($kg/m^3$) and $\dot{m}$ is the total release rate (kg/s).

The temporal boundary conditions needs to be specified by two main parameters during the simulations. These are the total mass flow of gas penetrating the surface, and the radius of the release area. It is found in a typical subsea release, that the mass flow from a transient pipeline rupture will reach a maximum mass flow through the surface at an early stage of the release, and that the radius of the release grows slower and reaches a maximum later. Effects such as the decay rate from the release, and water depth will influence this significantly and a generalization of the behaviour at the sea surface is not attempted here. If transient effects are significant, such as during a full bore rupture, it can be recommended to perform separate CFD simulations in order to generate the right starting conditions at the sea surface.

As a part of the present project, the FLACS and KFX CFD code developers wrote a special version of the codes with transient, circular source terms that can be specified as Gauss or Top hat profiles. For large, full bore ruptures, which are most relevant for transient releases, it is recommended to use these special boundary conditions in the codes.

Input in terms of radius and mass flow vs. time can be obtained by performing subsea CFD simulation where the subsea plume is modelled.

### 3.3 *Wind and turbulence inlet boundary conditions*

Together with the wind velocity 10 m above the sea, the surface roughness, $z_0$; and the Pasquill stability class are the main decisive parameters which describe wind and turbulence profiles.

Logarithmic velocity profile is recommended instead of the power law profile mainly because it is more flexible as it can represent the effects of the atmospheric stability and surface roughness. There are small differences in the default wind and turbulence profiles between FLACS and the KFX. The logarithmic wind profile and the turbulence profiles used in FLACS and KFX (Huser 1997) are recommended for use. These have the same behaviour of the eddy viscosity profile in the region up from the surface, to 20-30 m DNV (2009).

It is important to be aware that the inlet profiles of $k$ and $\varepsilon$ are decisive for the plume lengths in a CFD simulation when there are no turbulence generating obstacles and geometry elements in the domain. It is therefore recommended to verify that the resulting *eddy viscosity* upwind the subsea release is correct. Some examples of eddy viscosity profiles are given in DNV 2010 and DNV 2013. It is recommended to plot and validate the resulting eddy viscosity profile instead of separate profiles of $k$ and $\varepsilon$ in order to simplify comparisons. The eddy viscosity is a pure function of $k$ and $\varepsilon$.

#### 3.3.1 *Surface roughness*

For wind blowing over the open sea or ocean it is natural to use a low surface roughness, due to the sea being flat, and that the waves are most often following the wind resulting in an equivalent lower roughness. Most measurements of surface roughness are performed for wind over land, ranging from 1 mm as the lowest for flat, smooth surfaces (Blevins 1992). Values for the surface roughness are collected for a range of surfaces starting with the open sea in Blevins (1992) giving the interval: $z_0 = 0.0002$ m to 0.005 m for wind over the open sea. Research is continuing to obtain improved models for surface roughness above sea, and recently (Jenkins 2009) indicates surface roughness down to the order of $z_0 = 10^{-4}$ m with indication that it also can be lower. The surface roughness is dependent on the wind speed, but also the age of the sea and the wave lengths and wave direction, etc. The surface roughness is in general increasing with the wind speed due to the increasing wave size.

Based on the current knowledge of surface roughness above sea, it is suggested to use as a best practice the values given in Table 1. In Table 1, a linear relationship is applied between surface roughness

and wind speed, although more research is recommended (Jenkins 2009). These values are assumed to give conservative cloud lengths for most cases.

Table 1: Best practice roughness and stability class to be used for dispersion above sea in the wind boundary conditions. The variation in stability class for each table entry is due to different cloud cover. Less clouds gives more extreme stability classes, and more clouds gives stability class closer to neutral.

| **Wind speed 10 m above sea (m/s)** | **Roughness above Sea, $z_0$ (m)*** | **Pasquill class Unstable conditions** | **Pasquill class Stable conditions** |
|---|---|---|---|
| < 1.5 | $1.0 \cdot 10^{-4}$ | A, B | G |
| 1.5 to 3.5 | $1.5 \cdot 10^{-4}$ | A-B, C | F, G |
| 3.5 to 5.5 | $2.0 \cdot 10^{-4}$ | B, C | E, F |
| 5.5 to 6.5 | $2.5 \cdot 10^{-4}$ | C, D | D, E |
| 6.5 to 20 | $3.0 \cdot 10^{-4}$ to $1.0 \cdot 10^{-3}$ | C, D | D |
| 20 | $1.0 \cdot 10^{-3}$ | D | D |

* Typical values, lower surface roughness can occur.

### 3.3.2 *Atmospheric stability*

The stability is classified by Pasquill with letters A to C for unstable, D for neutral and E to G for stable. Neutral (Pasquill class D) and stable (class E, F, G) conditions give less turbulence and longer plumes, and it is therefore recommended to be used in risk assessment work. This will then be on the conservative side as both stable and unstable conditions can occur on the ocean. Also for stability, most of the measurements are performed for wind above land. Sorbojan (1989) gives the relationship between wind speed and stability class based on land observations. Similar trends are observed in Hasse (1985), which is valid for the sea. It is therefore recommended to use the wind speed with the stability classes given in Table1 1 when performing dispersion above sea simulations.

Table 2. Surface bubble zone radius for steady state plumes. From CFD simulations of subsea plumes.

| **Bubblezone radius (m)** | **Leak rate sea bottom (kg/s)** | | | | |
|---|---|---|---|---|---|
| **Depths (m)** | **10** | **30** | **100** | **300** | **1000** |
| **30** | *24* | | *24* | | |
| **65** | | *38* | | *36* | |
| **100** | *49* | | *56* | | *70* |
| **300** | | *65* | | *134* | |
| **400** | | | *73* | | *148* |

## 4 LOOK-UP TABLES AND PLUMEPRO PROGRAM

A look-up table for the surface flux and bubble zone radius at the sea surface based on the sea depth and leak rate at the sea bed is made by running the CFD model for subsea plumes. Table 2 show the bubble-zone radius for different subsea leak rates and water depths. Simulations with KFX have been performed with various surface fluxes, bubble zone radiuses, and wind speeds to create a look-up table for maximum plume lengths and heights above the sea surface for a buoyant gas.

These two sets of look-up tables are combined to find the resulting above sea plume extent based on the subsea release rate, water depth and wind speed. Interpolations in the look-up tables are used in the program PlumePro. The intermediate results are the bubble zone radius and surface gas flow rate; and the final results are the horizontal and vertical distances to the flammable (Lower Flammability Limit, LFL) concentration and to 50% of the flammable concentration (1/2 LFL), see Table 3.

Table 3. Example input and calculated results from PlumePro

| | | | Case 1 | Case 2 | Case 3 | Case 4 | Case 5 | Case 6 | Case 7 | Case 8 | Case 9 |
|---|---|---|---|---|---|---|---|---|---|---|---|
| **Input (validity range)** | | Unit | | | | | | | | | |
| Water depth, (0-400) | | (m) | 150 | 150 | 150 | 150 | 150 | 150 | 400 | 400 | 400 |
| Subsea leak rate, (0-3000) | | (kg/s) | 200 | 200 | 200 | 900 | 900 | 900 | 900 | 900 | 900 |
| Wind speed, (1-12) | | (m/s) | 1.5 | 5 | 12 | 1.5 | 5 | 12 | 1.5 | 5 | 12 |
| **Intermediate results on sea surface** | | | | | | | | | | | |
| Surface gas flow rate | | (kg/s) | 102 | 102 | 102 | 511 | 511 | 511 | 181 | 181 | 181 |
| Bubble zone radius | | (m) | 71 | 71 | 71 | 86 | 86 | 86 | 148 | 148 | 148 |
| **Output maximum plume dimensions** | | | | | | | | | | | |
| Max length | *L* (1/2 LFL) | (m) | 155 | 286 | 166 | 243 | 485 | 515 | 182 | 305 | 249 |
| | *L* (LFL) | (m) | 104 | 178 | 99 | 151 | 296 | 310 | 132 | 195 | 140 |
| Max height | *h* (1/2 LFL) | (m) | 91 | 20 | 4 | 232 | 66 | 12 | 119 | 21 | 2 |
| | *h* (LFL) | (m) | 61 | 10 | 2 | 154 | 42 | 7 | 60 | 11 | 1 |

## 5 CONCLUSIONS

A joint research program was carried out between DNV and SINTEF to develop a methodology for subsea and atmospheric gas dispersion.

The CFD subsea gas dispersion model was developed to simulate the plume and the free surface behavior resulting from subsea gas pipe rupture. The model captures the transient plume behavior, surface dynamics, subsea mass and heat transfer, whilst giving transient and stationary boundary conditions for dispersion above sea.

The CFD model for dispersion above sea accounts for the atmospheric boundary layer and gas source on the sea surface, and this paper gives the modeling guidance in order to achieve consistent results. Further details are given in a DNVs Recommended Practice (RP) which is being developed for the CFD modeling of dispersion above sea.

The two CFD models for gas dispersion below and above sea were applied with various subsea release rates and sea depths, surface fluxes, bubble zone radiuses and wind speeds to create look-up tables for maximum plume lengths and heights above the sea surface for a buoyant gas. The CFD generated look-up tables are integrated into a tool called DNV PlumePro where the height and distance to the LFL plume can be found given sea depth, release rate and wind speed. PlumePro interpolates in the look-up tables generated from a set of CFD modeling runs where the state-of-the- art modeling techniques are applied.

## 6 PREFERENCES


Blevins, R.D 1992 *Applied Fluid Dynamics Handbook* Krieger, 1992.

Briggs, G. A. 1969, *Plume rise*, U.S. Atomic Energy Commission, Clearinghouse for Federal and Technical Information, U.S. Bureau of Standards, Springfield, Virginia, TID-25075, 1969.

Cloete S., Eksteen, J.J. & Bradshaw, S.M., 2009, A mathematical modelling study of fluid flow and mixing in full scale gas stirred ladles", *Progress in Computational Fluid Dynamics*, **9**(No.6/7):345-356

Cloete S, Olsen, J.E. & Skjetne P., 2009, CFD modeling of plume and free surface behavior resulting from a subsea gas release." *Applied Ocean Research*, **31**, 220-225

DNV 2009, Dispersion Above Sea From Subsea Releases Phase 3 – A common CFD Model. *DNV report No.: 2009-1171, rev 0.*

DNV 2010. Dispersion Above Sea Phase 4 – Investigation of effects and Best practice manual. *DNV Report No.: 2010-0236, rev A.*

DNV 2011. Dispersion Above Sea from Subsea gas Releases, Phase 5. *DNV Report No.: 2011-1434, rev. 1.(open)*

DNV 2013 Subsea gas release and dispersion above sea: CFD modeling and PlumePro program. DNV Recommended Practice A-206. To be released 2013.

Engebretsen T., Northug T., Sjøen K. & Fanneløp T.K., 1997, Surface flow and gas dispersion from a subsea release of natural gas.", *Seventh Int. Offshore and Polar Engineering Conference*, Honolulu, USA

Gosman A.D. & Ioannides E., 1983, Aspects of computer simulation of liquid-fuelled combustors. *J.Energy*, **7**: p. 482-490

Hasse, L. & Weber, H., 1985. On the conversion of Pasquill categories for use over sea. *Boundary-layer Meteorology.* 31:177-185

Huser A., Nilsen J.P. & Skåtun H., 1997, Application of k-ε model to the stable abl: pollution in complex terrain, Journal of Wind Engineering and industrial Aerodynamics. 67 & 68 (1997) 425-436.

A.D. Jenkins 2009 Oversikt over hvordan havbølger påvirker vindprfilen og turbulens I atmosfæren. *Presentation held at the seminar: "Vindkraft FoU Seminar – fokus på offshore" Trondheim 22-23.01.2009.*

Skjetne P. & Olsen J.E., 2012, A parcel based modelling concept for studying subsea gas release and the effect of gas dissolution, *Progress in Computational Fluid Dynamics,* Vol. 12, Nos. 2/3

Sorbjan, Z. 1989 *Structure of the Atmospheric Boundary Layer* Prentice Hall, 1989.